Flexible Printed Gel Electrodes: Towards Living Plant Sensors for Nature-Based Environmental Monitoring

Gregory Whiting

Gregory.whiting@colorado.edu

University of Colorado Boulder https://orcid.org/0000-0003-2706-0233

Catherine Crichton

University of Colorado-Boulder

Taylor Shapre

University of Colorado Boulder

Heiko Kabutz

University of Colorado Boulder https://orcid.org/0000-0003-1060-9832

Elliot Strand

University of Colorado-Boulder

Nicholas Bruno

University of Colorado Boulder

Prashant Sankaran

University at Buffalo

Kaushik Jayaram

University of Colorado Boulder

Eloise Bihar

University at Buffalo

Article

Keywords: Bioelectrode, inkjet-printed, adhesive, hydrogel, electrophysiology

Posted Date: May 29th, 2025

DOI: https://doi.org/10.21203/rs.3.rs-6748528/v1

Additional Declarations: Yes there is potential Competing Interest. Authors Bihar, Strand, and Whiting are authors on a patent application submitted by the University of Colorado Boulder related to findings described in this manuscript.

Version of Record: A version of this preprint was published at Communications Engineering on March 19th, 2026. See the published version at https://doi.org/10.1038/s44172-026-00638-z.

Flexible Printed Gel Electrodes: Towards Living Plant Sensors for Nature-Based Environmental Monitoring

Catherine A. Crichton[1], Taylor Sharpe[1], Heiko Kabutz[1], Elliot J. Strand[1], Nicholas Bruno[1], Prashant Sankaran[2], Kaushik Jayaram[1], Eloïse Bihar[3], Gregory L. Whiting[1*]

[1*]Paul M. Rady Department of Mechanical Engineering, University of Colorado Boulder, 1111 Engineering Drive, Boulder, 80309, CO, USA.
[2]Department of Industrial and Systems Engineering, University at Buffalo, 307 Bell Hall, Buffalo, 14260, NY, USA.
[3]Department of Materials Design and Innovation, University at Buffalo, 120 Bonner Hall, Buffalo, 14260, NY, USA.

*Corresponding author(s). E-mail(s): gregory.whiting@colorado.edu;
Contributing authors: catherine.crichton@colorado.edu; tash2618@colorado.edu; heiko.kabutz@colorado.edu; elliot.strand@colorado.edu; nicholas.bruno@colorado.edu; psankara@buffalo.edu; kaushik.jayaram@colorado.edu; eloisebi@buffalo.edu;

Abstract

Interfacing bioelectronic devices with plants can enable nature-based sensing networks through transduction of self-generated electrical signals from living plant nodes into real-time environmental data. A key challenge in developing such platforms is to create stable, biocompatible electrodes that provide sufficient adhesion to plant tissue with minimal impedance drift. In this report, an adhesive gel electrode featuring an inkjet-printed poly(3,4-ethylenedioxythiophene) polystyrene sulfonate (PEDOT:PSS) trace on a poly(vinyl alcohol) (PVA) hydrogel substrate with a methyl cellulose adhesive is presented. When attached to the inside of a Venus flytrap (*Dionaea muscipula*) lobe these biocompatible printed conformable electrodes demonstrate long-term mechanical stability and reliable continuous recording of action potentials. Compared to commercial Ag/AgCl electrodes, the developed bioelectrodes provide higher sensitivity, faster signal

dynamics, and comparable signal-to-noise ratios. The adhesive gel electrodes maintain low impedance over extended periods, which is critical for long-term monitoring bioelectronic signals. Low impedance and robust connection to the plant tissue enabled the tracking of diurnal changes. This stability enabled real-time monitoring of a Venus flytrap's response to environmental factors such as temperature variations and insect activity. Additionally, the bioelectrodes were integrated with low-cost ESP32 microcontroller-based electronics, enabling wireless plant-to-plant communication over long distances. This system demonstrates a biologically integrated platform for developing nature-integrated networks that utilize living plants as sensor nodes.

Keywords: Bioelectrode, inkjet-printed, adhesive, hydrogel, electrophysiology

1 Introduction

Advances in bioelectronic technologies have enabled the integration of electrodes with living tissues to advance human healthcare[1–3]. More recently, similar strategies have been applied to plants, where bioelectronic devices are used to monitor physiological signals for use in agriculture and environmental monitoring, building platforms for smart farming practices[4–7]. This method of sensing directly monitors plant health and their responses to environmental stimuli such as photosynthesis, drought stress, and wounding, as well as monitoring electrical signaling[8–10]. Plants utilize electrical signaling to enable long-distance communication between cells[11–13], which plays a crucial role in their ability to sense and respond to stimuli such as touch[14–16], herbivore-induced wounding[17, 18], light exposure[19, 20], and temperature fluctuations[14, 21, 22]. These electrophysiological signals are inherently self-generated and provide real-time feedback on complex environmental stimuli. When harnessed with stable and conformal electrodes, these electrical signals can be transduced to create a nature-based sensing network, where each plant serves as a responsive node for real-time distributed sensing. A primary issue in monitoring plant electrophysiology, however, has been the challenge of creating biocompatible and robust electrodes capable of recording and stimulating plant electrical activity over extended periods of time[23, 24]. Certain touch-sensitive plants, such as the Venus flytrap (*Dionaea muscipula*, VFT) and the *Mimosa pudica*, are capable of producing electrical signals that trigger thigmonastic movements, allowing them to serve as models for studying plant electrophysiology and developing a platform for biological integrated sensor networks[25]. The VFT serves as an excellent model for plant electrophysiology due to its well-characterized and reproducible action potentials (APs), which are generated in response to the stimulation of mechanosensitive trigger hairs inside the lobes of the trap[25, 26], where two hairs are stimulated to produce APs within 20 s, the stimulated lobes of the VFT will close[27].

Though widely used, conventional Ag/AgCl electrodes are bulky, invasive, and poorly suited for long-term interfacing on plant tissues, such as the inside of VFT

lobes[28–30]. In order to address this issue, studies have explored conformable electrodes, focused on monitoring and applying APs from outside the VFT lobes. Action potentials have been successfully recorded for short durations, but sustained adhesion to plant tissues and operation over extended time periods remains an important challenge[29, 31]. In this work, we present an adhesive bioelectrode that integrates inkjet-printed PEDOT:PSS traces with a poly(vinyl alcohol) (PVA) hydrogel substrate specifically designed to adhere to plant tissues such as the inner surface of a VFT lobe using a thin layer of methyl cellulose (MC). The adhesive gel electrodes enable conformal and stable recording of plant electrophysiology that forms the foundation for a biologically integrated environmental sensing platform. Compared to Ag/AgCl electrode alternatives, the gel electrodes exhibit excellent biocompatibility as they do not induce necrotic tissue formation after continuous contact over many days, and show enhanced long-term performance with minimal impedance change when measured over 120 hrs. The adhesive gel electrodes are also capable of monitoring environmental variables, such as diurnal cycling, insect activity, and temperature fluctuations, and can deliver electrical stimulation to close the lobes of other VFT plants remotely.

This research presents a novel approach to integrate bioelectrodes with a VFT's natural sensing capabilities to create a living environmental sensor. The adhesive gel electrodes adhere directly to the plant tissue, allowing long-term monitoring of the plant's electrophysiology as it responds to its environment. Changes in environmental variables, such as light intensity, relative humidity (RH), and vapor pressure deficit (VPD), resulted in changes to the plant's impedance and enabled the tracking of diurnal cycles, emphasizing the platform's ability to function as a biohybrid sensor. Temperature variations, such as cooling to ∼9 °C, also generated APs, which were reliably detected using the adhesive gel electrodes. The electrode's mechanical stability also allowed them to record APs generated from plant-insect interactions. These electrodes can be paired with off-the-shelf wireless electronics to enable plant-to-plant communication across long distances. The integration of conformal gel electrodes with wireless electronics that transduce electrophysiological signals from plants paves the way for developing intelligent, self-sustaining, nature-based sensor networks.

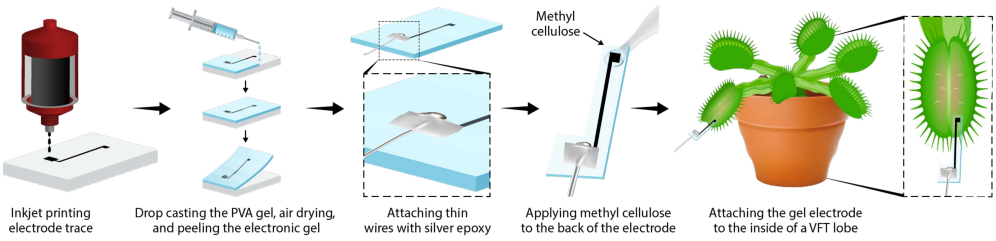

Fig. 1 Fabrication steps for manufacturing and adhering the gel electrode platform onto the inner surface of a Venus flytrap lobe.

2 Results and Discussion

2.1 Printed Electrode Optimization

PEDOT:PSS traces were first ink-jet printed and then transferred to a flexible, uncrosslinked PVA substrate (Figure 1) to act as gel electrodes for plant electrophysiological monitoring. The three inkjet-printed layers that made up each trace were deposited using a Dimatix DMP-2800 inkjet printer using wet-on-wet printing onto a glass slide, then dried on a hot plate at 90 °C under ambient conditions for 10 min. Once dried, the PVA layer was drop-cast on top of the traces and left to dry for 24 hours under ambient conditions. The electrodes were then peeled off the glass slide, and a thin wire was attached using silver epoxy. To evaluate the performance of the gel electrodes, which were adhered to the plant tissue using methyl cellulose, we compared their biocompatibility, adhesion, and long-term stability, which are all crucial for continuous electrophysiological monitoring, against Ag/AgCl wire electrodes. The adhesive gel electrodes showed improved biocompatibility compared to the commercial electrodes, as seen in Figure 2a, over nine days. The bioelectrodes did not cause any visible necrosis or tissue damage on the lobe, while the commercial electrodes caused significant amounts of necrotic tissue. This tissue damage suggests that the commercial electrode was cytotoxic to the plant when in contact with the tissue over extended periods.

Due to their small size, the adhesive electrodes were able to be adhered to the inside of the lobe, using methyl cellulose applied to the PVA gel and then placed onto the plant tissue near the bases of the mechanosensitive trigger hairs. In contrast, the Ag/AgCl wire electrodes needed to be placed in contact with the outside of the flytrap's lobe as they could not be placed on the inside of the lobes due to their size, which frequently stimulates the trigger hairs, causing the closure of the lobes. The commercial electrodes relied on a gel to maintain constant contact with the plant tissue. However, due to their inability to adhere to the plant tissue, these electrodes easily lost connection due to mechanical perturbation. This loss of connection occurs as the Ag/AgCl wire electrodes rest against the plant tissue, unadhered, while the gel electrodes are physically adhered to the plant tissue using methyl cellulose. A tensile test was conducted to analyze the properties of the adhesive electrode under uniaxial tension. The electrode was adhered to a glass slide using a thin layer of methyl cellulose, was left to dry for an hour, and then tested using an MTS Insight II Material Testing System (Figures 2b-c). The interfacial shear modulus of the adhesive gel/-glass interface was ∼19 kPa, showing that the adhesive can withstand deformations without failing. The bioelectrode began to delaminate from the glass slide at a strain of 10% and a shear stress of 145 kPa. During delamination, the average shear stress was 153 kPa ± 7 kPa. The electrode fully delaminated at a strain of 47%, demonstrating that the electrode is mechanically robust enough to maintain contact with the plant tissue under moderate stress. The long-term stability of the commercial and the printed adhesive gel electrodes was also evaluated using electrochemical impedance spectroscopy (EIS). A commercial Ag/AgCl wire electrode was placed in contact with one lobe of a plant, while the adhesive electrode was attached to the inside of a lobe of another leaf on the same plant. The commercial and adhesive electrodes were attached

to a common counter electrode, a needle in the hydrated sphagnum moss growing media (Figure 2d). The commercial electrode exhibited a ∼30x increase in impedance modulus at 1 kHz over the course of the experiment (120 hrs). In contrast, the adhesive gel electrode maintained a relatively stable impedance profile over the same period with a ∼1x increase in impedance (Figure 2e). Environmental variables for the duration of the experiment were collected using a Pulse Pro environmental data logger (environmental variables plotted in Supplementary Figures 3-9). The Pearson correlation coefficients (r) between the environmental variables and the impedance modulus at 1 kHz for both the adhesive and commercial electrodes were calculated (Table 1), using Equation 1.

$$r = \frac{\sum (x - \bar{x})(y - \bar{y})}{\sqrt{\sum (x - \bar{x})^2}\sqrt{\sum (y - \bar{y})^2}} \tag{1}$$

Although both electrodes demonstrated susceptibility to drying (r = -0.80 and r = -0.88 for the adhesive and commercial electrodes respectively, with respect to dew point), impedance correlations revealed that the adhesive electrode demonstrated enhanced stability against drying under environmental conditions with a moderate negative correlation to relative humidity (RH) (r = -0.43) and negligible correlation to vapor pressure deficit (VPD) (r = -0.12). The commercial Ag/AgCl electrode, however, was sensitive to drying and had a strong negative correlation to RH (r = -0.79) and a moderate positive correlation to VPD (r = 0.43), leading to large increases in impedance over time. Changes in the RH and VPD minimally impacted the adhesive gel electrode, showing that they are more stable for long-term electrophysiological monitoring. A moderate negative correlation (r = -0.47) between ambient light intensity (lux) and the impedance at 1 kHz with the adhesive electrode, demonstrating a capacity to track diurnal cycles. The diurnal cycling can be seen in the impedance fluctuations during the day/night cycles in Figure 2e as the plant undergoes changes in photosynthetic activity[32–34]. The Ag/AgCl electrode was unable to track the plant's diurnal cycling and had a negligible correlation to light intensity (r = -0.03).

2.2 Action Potential Recording and Electrical Stimulation

To evaluate the ability of the adhesive gel electrodes to record APs in VFTs reliably, we used the electrodes to record APs generated from manual stimulation of the trigger hairs using a wire (Figure 3a, 3b) and performed an analysis of the resulting signals. The recorded APs were processed as follows. First, we resample the potentials to ensure a constant time interval of 1 ms. Then, a Savitzky-Golay filter with a window length of 65 fitted by a first-order polynomial is applied. The adhesive gel electrodes' performance was compared to the commercial Ag/AgCl electrodes. The bioelectrodes had a similar signal-to-noise ratio (SNR) as the commercial electrodes, which was determined from the data before applying the Savitzky-Golay filter. An Oneway Welch ANOVA testing for equal means with potentially unequal variances was performed between the SNR for the bioelectrode (n = 12) and the Ag/AgCl electrode (n = 13), resulting in a p-value of 0.0032, suggesting a trend toward the bioelectrodes having a

Table 1 Pearson correlation coefficients between the impedance modulus at 1 kHz of adhesive gel electrodes and commercial electrodes and environmental variables.

Environmental Variable	**Adhesive Gel Electrode** Impedance (Ω)	**Commercial Electrode** Impedance (Ω)
Light Intensity (Lux) Range: 0–77.75 Lux Avg: 34.00 Lux ± 33.12 Lux	-0.47	-0.03
Relative Humidity (%) Range: 15.61%–29.24% Avg: 22.54% ± 3.36%	-0.43	-0.79
Vapor Pressure Deficit (kPa) Range: 1.74–2.62 kPa Avg: 2.10 kPa ± 0.22 kPa	-0.12	0.43
Dew Point (°C) Range: −3.73°C–2.67 °C Avg: −0.38 °C ± 1.65 °C	-0.80	-0.88

higher SNR than the commercial electrodes (Figure 3c). The Welch's Test also demonstrated that the bioelectrodes recorded significantly higher average amplitudes of the APs compared to the commercial Ag/AgCl wire electrodes (64.3 mV ± SE 2.7 mV vs. 37.5 mV ± SE 2.6 mV, $p < 0.0001$, Figure 3e). The difference indicates that the adhesive electrodes have enhanced sensitivity and improved performance when recording APs. The analysis also showed that APs recorded with the adhesive electrodes have a significantly shorter average full-width at half maximum compared to the commercial Ag/AgCl wire electrodes (891 ms ± SE 63 ms vs. 620 ms ± SE 61 ms, Welch's Test, $p = 0.0050$, Figure 3g). The decreased recorded amplitude and increased FWHM while using the commercial electrode are likely due to signal distortion caused by poor connection to the plant tissue, a limitation effectively mitigated with the bioelectrode due to its ability to adhere effectively to the lobe[29, 31]. The robustness of the adhesive gel electrodes was also demonstrated through an experiment where an electrode was attached for recordings and then removed each day over 14 days. Over the course of the long-term experiment where the electrodes were removed and reattached, the recorded APs had an average amplitude of 48.0 mV ± SE 1.5 mV, an average FWHM of 851 ms ± SE 26 ms, and an average signal-to-noise ratio of 24.2 dB ± SE 0.8 dB (Figure 3d) with a statistically significant difference between signal and noise levels (Wilcoxon Signed Rank test, $p < 0.0001$). The averaged amplitude and FWHM collected during the long-term experiment align with the baseline values collected while comparing the bioelectrodes to the commercial Ag/AgCl electrodes. The stable SNR and minimal variability in the amplitude and FWHM of the APs recorded during the 14-day experiment support the bioelectrodes' mechanical robustness and ability to adhere to the plant tissue.

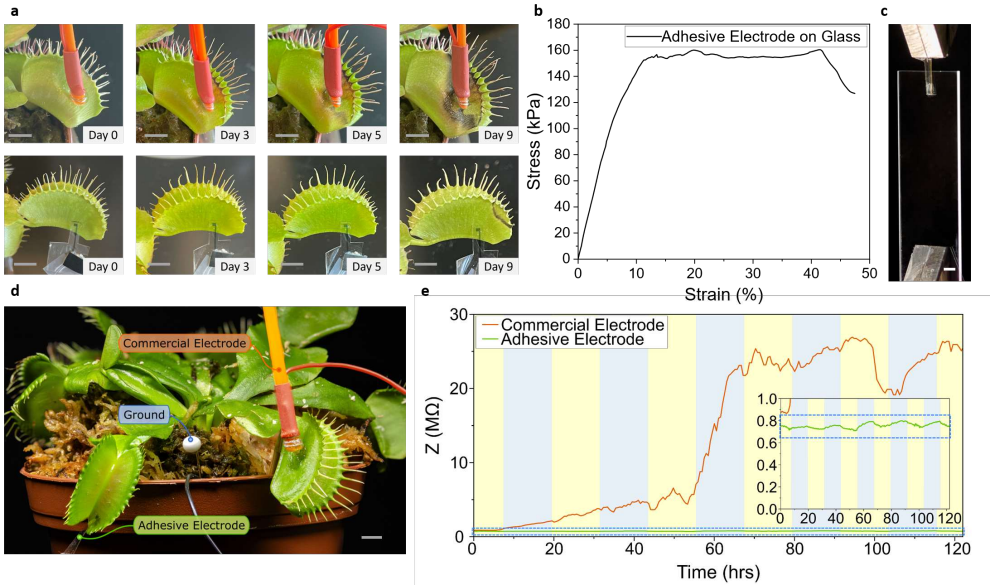

Fig. 2 (a) Photographs of a commercial electrode and a bioelectrode attached to the outside of VFT lobes for 9 days (scale bars are 5 mm). (b) A stress-strain plot of a bioelectrode adhered to a glass slide with methyl cellulose under uniaxial tension and (c) a photograph of the electrode adhered to the glass slide before stretching (scale bar is 5 mm). (d) A photograph of the electrode configuration for the long-term electrochemical impedance spectroscopy (EIS) experiment (scale bar is 5 mm) and (e) the impedance modulus at 1 kHz for the commercial and adhesive gel electrodes as a function of time.

A mechanically stimulated AP was extracted from a VFT and amplified to have a voltage of -20 V applied via a Keithley 2600 source-measure unit (SMU) to electrically stimulate VFTs to induce them to close. The electrical stimulation was delivered via an adhesive electrode attached to the inside of a lobe near a trigger hair, and a needle was placed in the hydrated sphagnum moss growing media. Lower stimulation voltages ($\leq$15 V) failed to induce lobe closure reliably, likely due to the impedance of the bioelectrode-plant tissue interface. A stimulation voltage of $\pm$20 V was sufficient to cause the VFT lobes to close reliably. The applied signal was also monitored using another adhesive electrode that was adhered to the inside of the VFT lobe. APs delivered with a 15 s gap between them were sufficient to cause the lobes of the VFT to close. As shown in Figure 4, the VFT remained open after the first applied AP (t_2) but began to close after the second applied AP (t_3), which caused it to close fully (t_4) (Figure 3f and Supplementary Video 1).

2.3 Plant-to-Plant Communication

Building on the electrodes' ability to record and electrically stimulate APs reliably, we integrated the adhesive gel electrodes with low-cost wireless electronics to enable plant-to-plant communication. This system reliably records APs and electrically stimulates VFTs to induce trap closure at a distance tested up to 45 m. While this has

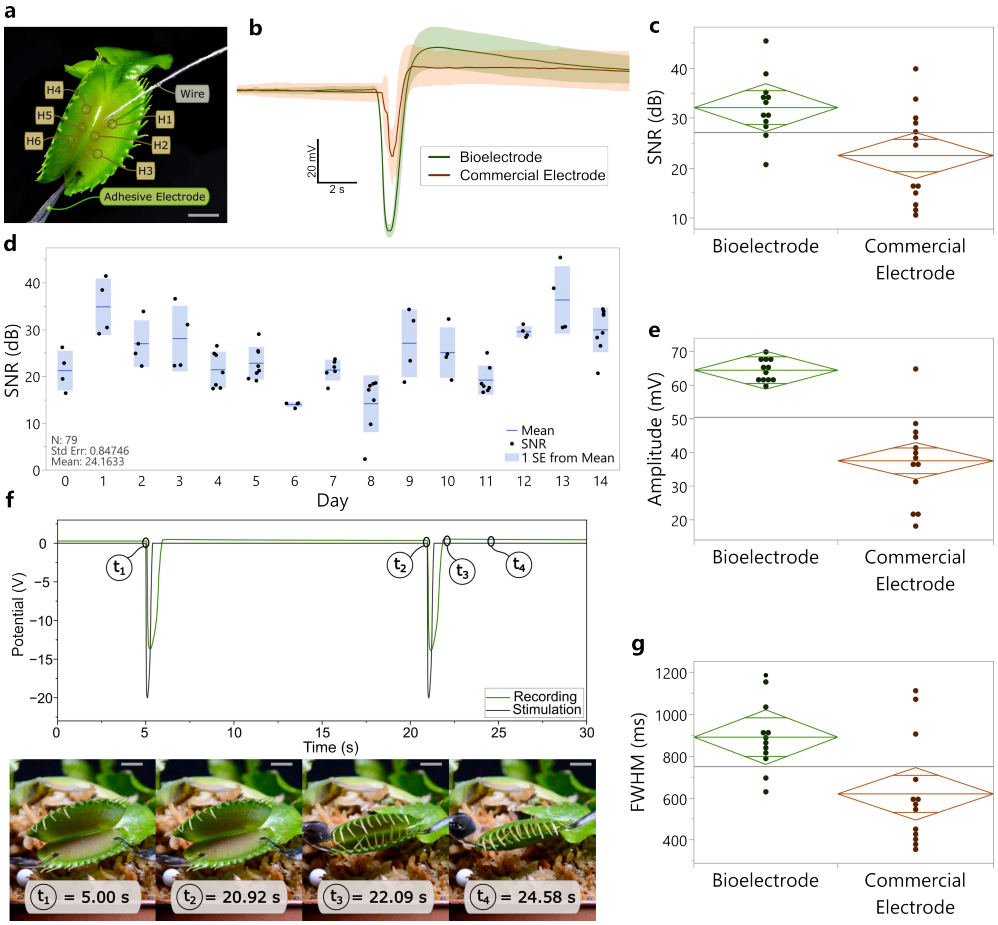

Fig. 3 (a) Photograph of VFT with adhesive gel electrode adhered to the inside of a lobe with a wire in position to deliver mechanical stimulation to generate an AP with all trigger hairs identified (scale bars are 5 mm). (b) The average and standard deviation of the action potentials for the bioelectrode and the commercial electrode used in the analysis. (c) The signal-to-noise ratio of the AP signals for the bioelectrode and the commercial electrode. (d) The signal-to-noise ratio for an adhesive gel electrode that was removed and attached to a VFT over 14 days. (e) The amplitude of APs recorded using the bioelectrode and the commercial electrode. (f) Plot of applied electrical stimulation and recorded response from gel electrodes adhered to the inside of a VFT lobe and grounded through a needle in the sphagnum moss growing media, and images of the plant receiving electrical stimulation and closing (scale bars are 5 mm). (g) The FWHM of APs recorded using the bioelectrode and the commercial electrode.

previously been achieved in controlled settings using laboratory-grade electronics, we implemented a low-cost, printed electronics-based approach to monitor and stimulate plant electrical signals. Two additional contributions are described here: the use of low-cost microcontrollers to detect unamplified AP signals and deliver electrical stimulation, and a demonstration of mirrored plant activation at a distance. In prior literature, instruments have been used to detect and apply APs to individual plants[35–37]. Here, two identical ESP32 microcontrollers (Figure 4a) were used

to detect, transmit, and apply APs from a transmitter plant to a receiver plant located 15 m apart (Figure 4b); other tests were also conducted with a maximum of 45 m separation. The microcontrollers communicated over the ESP-NOW protocol (Espressif Systems) using on-board PCB antennas. This protocol supports up to 10 encrypted peers, packet sizes up to 250 bytes, a range of over 200 m, and low transmission latency. Both boards were powered with independent 3.7 V Lithium-polymer batteries. Firmware was written using the Arduino IDE. For the transmitter microcontroller, an analog input GPIO pin was connected to the plant's printed electrode, a GPIO ground pin was connected to a pin grounded in the sphagnum moss growing media, and analog voltage readings were taken continuously at a frequency of 48 Hz. Two data signal processing algorithms were used in the transmitter firmware to allow for sensitive event detection with low-cost electronics: first, noise was reduced from analog readings by rapidly taking 10 analog input readings, calculating the average deviation in the signal, and filtering out any readings that fell outside of that deviation. This filtered out noise associated with the ADC. Second, new readings were written to adjustable arrays sized to detect sustained changes in voltage below an adjustable threshold, compared to a baseline array, which is updated in real time. This approach prevented single or sporadic readings from triggering an event, requiring several sequential readings below the threshold to determine that an event had occurred. Observed APs were used to determine the magnitude and duration of signal change associated with events; in the firmware used, the voltage threshold was set to 20 mV below baseline, and to be considered an actual event, four sequential readings had to be detected below that threshold. The receiver was similarly connected to a plant with a voltage regulator output pin connected to the electrode, and the GPIO ground connected to a needle in the sphagnum moss growing media. On detection of an event, the transmitter sends a packet containing a pulse duration command to the receiver. Based on observations of logged APs, a pulse length of 3 s was selected for this experiment. On receipt of a packet, the receiver enabled a 20 V voltage regulator (Pololu Robotics) for the duration sent in the transmitted packet. The regulator applied a square-wave pulse to the electrode on the receiver plant, simulating an AP. For ease of use, the receiver and transmitter provided visual and audio feedback via an onboard LED and a piezo buzzer when events were detected on the transmitter side or received on the receiver side. The ability of this low-cost system to wirelessly mirror APs between two instrumented plants placed 15 m apart and independently powered was demonstrated. Manual stimulation of the sensory hairs on the transmitting plant were detected as events by the attached microcontroller (Figure 4c), which transmitted a command to the receiving microcontroller, applying a 3-second, 20 V pulse to the receiving plant (Figure 4d). Two events were recorded and transmitted, resulting in both plants closing (Supplementary Video 2).

2.4 Environmental Monitoring

The ability of the VFT monitored with adhesive gel electrodes to function as an environmental sensor was tested using two primary stimuli: mechanical stimulation via insect interactions, and APs induced due to temperature changes. VFTs with gel electrodes adhered to the inside of their lobes were placed inside an enclosure where

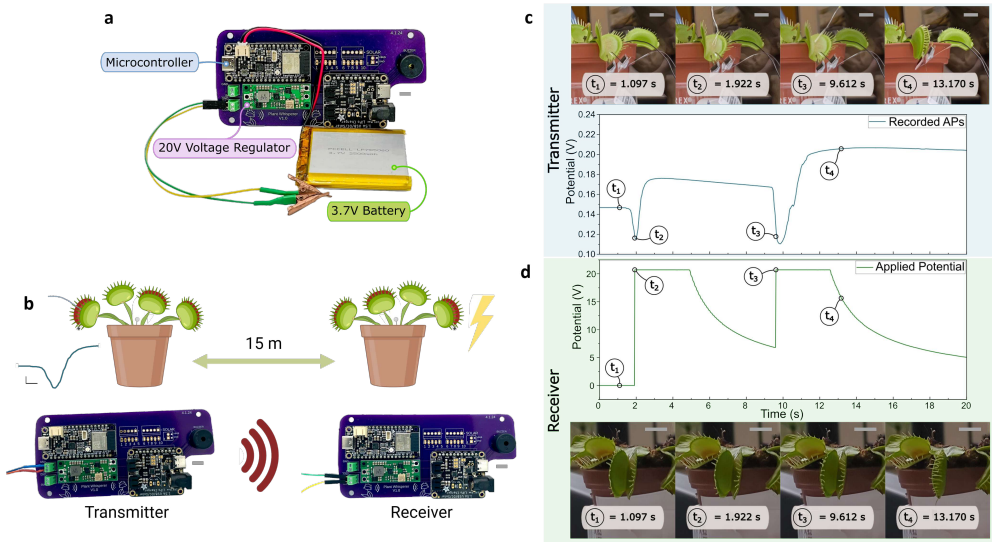

Fig. 4 (a) The labeled components of the transmitter and receiver electronics (scale bar 5 mm). (b) Illustration of plant-to-plant communication at a distance of 15 m with pictures of the electronics for the transmitter and receiver (AP y scale bar is 10 mV, AP x scale bar is 0.25 s; transmitter and receiver scale bars are 10 mm) (c) The transmitter microcontroller is attached to a printed adhesive gel electrode grounded through a needle in the sphagnum moss growing media and transmits a packet when an event is detected from the transmitter plant, stimulated by hand (scale bars are 10 mm). (d) An identical microcontroller, the receiver microcontroller, is connected to a printed electrode attached to the plant and grounded through a needle in the sphagnum moss growing media (scale bars are 10 mm). Upon receiving a packet, a 20 V voltage regulator is enabled for a pulse length determined by the packet content, simulating an AP for the receiver plant.

large crickets (*Acheta domesticus*) were introduced and allowed to move freely (Figure 5a). Occasionally, the crickets stimulated the VFT's sensory trigger hairs, generating APs. These APs were recorded in real-time using an electrode that was adhered to the inside of the VFT's lobe and a needle located in the hydrated sphagnum moss growing media and connected to a Keithley DMM6500 multimeter. The crickets were able to mechanically stimulate the trigger hairs to generate APs without closing the VFT, APs in close enough proximity to close the VFT but without capturing the cricket, and APs that would close the VFT and capture the cricket. If a cricket was captured, it would generate a substantial number of APs from inside the lobes after the plant had closed (Figure 5b and Supplementary Video 3). In the VFT experiments involving crickets, the recorded APs were preprocessed similarly, as described in section 2.2. The preprocessed APs were binned into different events of interest (Baseline, Closed, Closed But No Capture, Post Close, and Random) and analyzed using a one-way analysis of variance (ANOVA) for each response variable: amplitude and FWHM. The ANOVA results (Supplementary Figure 10) indicate that the events have a significant effect on the two response variables (amplitude $p < 0.0001$ and FWHM $p < 0.0001$). Further, a post-hoc non-parametric all-pair analysis was performed using the Steel-Dwass method, which effectively accounts for uneven samples per event. The post-hoc analysis results show that the amplitude for the post close events ($46.0 \pm$ SE

1.2, n=46) was significantly different than the baseline events ($35.4 \pm$ SE 2.3, n=12, $p = 0.0166$), while the remaining comparisons were insignificant. The FWHM for the post close events ($1312 \pm$ SE 39, n=46), were significantly different from the baseline events ($678 \pm$ SE 76, n=12, $p < 0.001$), Closed events ($63.8 \pm$ SE 132, n=4, $p = 0.0120$), and random events ($551 \pm$ SE 152, n=3, $p = 0.0347$). Overall, the APs for the Post Close events had higher amplitudes and FWHM than the baseline, manually triggered, events.

Another environmental factor that causes AP generation is cold shock[38]. Cold shocking depolarizes membrane potentials similar to the response observed during mechanical stimulation of the trigger hairs[38, 39]. To assess the adhesive gel electrode's ability to monitor the VFT's response to temperature, plants were placed in a freezer initially at room temperature. The freezer was then cooled gradually (Figure 5c). Once the temperature reached $9.0\,^{\circ}\mathrm{C} \pm 0.7\,^{\circ}\mathrm{C}$ (n=3), spontaneous APs occurred within the VFTs, causing the lobes to close (Figure 5d and Supplementary Video 4). The APs were preprocessed similarly, as described in section 2.2. However, apart from binning the different events of interest (baseline AP, freezer AP, freezer AP - closed) as done for the cricket experiment, we also include the temperature data for different APs. We chose a least squares fit regression analysis (Supplementary Figures 11-15) to study the effect of the different events (categorical variable) and temperature (continuous variable). The results reveal that the effects of temperature and events on FWHM are significant ($p < 0.0001$ and $p = 0.0095$) while insignificant for amplitude ($p = 0.2765$ and $p = 0.4814$). Additionally, an ad-hoc Tukey-Kramer Honestly Significant Difference (HSD) multiple comparison test was performed for the different events. The results indicate that FWHM for baseline significantly differs from freezer AP - closed ($p = 0.0156$), while other comparisons were insignificant ($p > 0.1$). Also, the all-pairs comparison of events on the amplitude measure was insignificant for all combinations ($p > 0.47$). The results from both the insect interaction and temperature sensitivity experiments highlight the adhesive gel electrode's ability to monitor bioelectronic signals of the VFT's response to environmental changes.

3 Conclusion

In this work, we demonstrate the ability of an inkjet-printed PEDOT:PSS on a soft PVA-gel substrate to adhere to the inside of VFT lobes using a methyl cellulose adhesive layer. These electrodes exhibit mechanical robustness through a stable impedance over extended periods, and their ability to adhere to the plant tissue without cytotoxic effects enables longer-term electrophysiological monitoring and stimulation in VFTs when compared with rigid Ag/AgCl electrodes. An Oneway Welch ANOVA test found that the bioelectrodes had a comparable SNR to the commercial electrodes, and the recorded signals from the adhesive electrodes demonstrated a higher average amplitude and average FWHM, indicating that the bioelectrodes provided enhanced signal when compared with the rigid electrodes. The bioelectrodes also demonstrated robust operation by being removed from the plant and reattached over the course of 14 days while maintaining a consistent SNR, amplitude, and FWHM for the recorded APs.

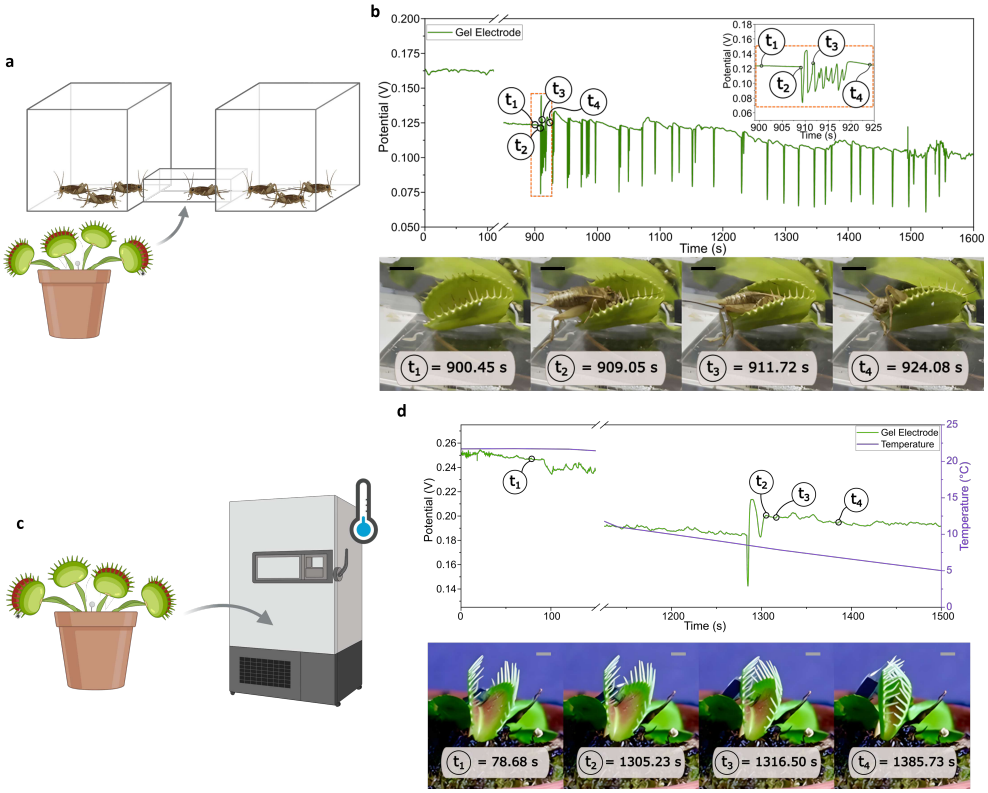

Fig. 5 (a) Illustration of VFT being introduced to an enclosure of crickets and (b) the recorded potential of a VFT capturing a cricket with additional action potentials generated from the trapped cricket (scale bars are 5 mm). (c) Illustration of VFT being put inside a freezer and (d) the recorded potential of a VFT and temperature in a cooling freezer (scale bars are 5 mm).

These values, averaged over the long-term experiment, are in line with baseline values. The soft adhesive electrodes can repeatedly deliver electrical stimulation on the order of ±20 V to close the lobes of the VFT, and can be paired with low-cost electronics to enable wireless plant-to-plant communication, stimulating a plant to close, which triggers another plant located some distance away to also close. The adhesive gel electrodes provided real-time feedback on the VFT's responses to environmental stimuli such as insect activity. A Steel-Dwass post-hoc analysis revealed that the APs recorded post-closure had significantly higher amplitude and FWHM than the baseline manually triggered APs. A least squares fit regression analysis revealed that the effect of temperature on FWSM for APs is significant, and a Tukey-Kramer HSD post-hoc analysis revealed that the FWHM for baseline manually triggered APs significantly differed from freezer-induced AP at closure. This work demonstrates the potential of these biocompatible printed adhesive gel electrodes for long-term stable interfacing with plant tissues, and the possibility of their use to enable plants to act as living, biohybrid environmental sensors that use natural electrophysiological responses for real-time monitoring for nature-based sensor networks.

4 Materials and Methods

4.1 Materials and Ink Formulation

PEDOT:PSS Clevios™ F.H.C. ink was purchased from Heraeus. PEDOT FHC was mixed with 1 wt.% of glycidoxypropyltrimethoxysilane (GOPS, Sigma Aldrich) to crosslink the PEDOT:PSS conductive trace[**?**]. The PEDOT:PSS ink concentration was 1-1.5%, and its viscosity was 8-70 mPa s before the GOPS was added. The PEDOT:PSS inks were sonicated in an ultrasonic bath for 30 min and filtered using a 1.2 μm PTFE filter. For the substrates and the adhesive, PVA (M_w 89,000-98,000 g mol^{-1}; Sigma Aldrich), phosphoric acid (Sigma Aldrich) for better transfer of the PEDOT:PSS from the glass slide, methyl cellulose (Sigma Aldrich), and deionized water were used.

4.2 Device Fabrication

Each layer was deposited using a Dimatix DMP-2800 inkjet printer with a 10 μm drop spacing, using wet-on-wet printing on a glass substrate for a total of three layers[4**?**]. The printer plate temperature was kept at 50 °C and the ink at 30 °C. After printing, the conducting traces were dried on a hot plate at 90 °C under ambient conditions for 10 min. PVA gels (100:10 water:PVA ratio, M_w = 89,000-98,000 g mol^{-1}) were prepared by dissolving PVA in deionized water at 90 °C under magnetic stirring. Methyl cellulose was prepared by dissolving methyl cellulose (deionized water : methyl cellulose weight ratio 30:1) in deionized water on a hot plate at 90 °C using magnetic stirring. For the electronic adhesive gels, after curing the conducting electrode, a layer of PVA gel was deposited and dried for 24 h at room temperature. The device was then peeled, thin wires were attached using silver epoxy (MG Chemicals 8331D), and left to dry for 12 hrs at room temperature. Once dried, T-Rex tape (purchased from Home Depot) was applied over the silver epoxy/PVA junction. When attaching the electrodes to the VFTs, a thin layer of methyl cellulose was added to the PVA to act as an adhesive to attach the electrode pad (1 mm x 1.5 mm) to the plant.

4.3 Commercial Electrodes

The commercial electrodes were purchased from Backyard Brains as part of their Plant SpikerBox and consisted of an Ag/AgCl wire wrapped around a plastic rod. SignaGel electrode ionic gel (purchased from Backyard Brains) was used as a conductive electrolyte between the commercial electrode and the plant tissues.

4.4 Characterization of Adhesive Gel Electrodes

4.4.1 Electrical Characterization

Electrochemical impedance spectroscopy (EIS) was performed using an EmStat Pico (Palmsens) impedance analyzer over a frequency range of 22 Hz to 200 kHz with a 100 mV applied potential. Action potentials were monitored using a Keithley DMM6500 multimeter.

4.4.2 Mechanical and Adhesion Testing

An MTS Insight II electromechanical testing machine was used to perform the mechanical characterization of the electronic gel-based devices and their adhesion to glass slides under uniaxial tension at a rate of 30 mm min^{-1}. A 250 N load cell was used for the experiments.

4.5 Electrophysiological Experiments

4.5.1 Action Potential Monitoring

All action potentials (APs) were monitored using a Keithley DMM6500 multimeter, with voltage recorded between a bioelectrode adhered to the inside of the VFT lobe and a needle that was inserted into the hydrated sphagnum moss growing media. The Keithley DMM6500 collected data at a sampling rate of 60 Hz. No additional signal processing, filtering, or noise rejection methods were applied. A wire was used to manually touch a sensory trigger hair to stimulate an AP. To prevent premature closing of the lobes while collecting APs, a 2 min waiting period between mechanical stimulation attempts was implemented.

4.5.2 Electrical Stimulation and Plant-to-Plant Communication

Electrical stimulation was delivered through the gel electrodes using a Keithley 2600 source-measure unit (SMU) and a 20 V voltage regulator (Pololu Robotics). For experiments conducted using the Keithley SMU, a recorded AP was amplified to have a minimum of -20 V, which was then applied to the VFT twice with a 15 s interval. Electrical stimulation using the 20 V voltage regulator was initiated using a set of two ESP32 microcontrollers (Adafruit, Inc.), which were used to detect, transmit, and apply APs between a transmitter and receiver plant, tested at a maximum of 45 m, apart using the ESP-NOW protocol to enable plant-to-plant communication. The transmitter microcontroller, connected to a plant electrode, sampled voltage at 48 Hz and employed a two-step signal processing algorithm to filter noise and detect sustained voltage drops of at least 20 mV below baseline. When an event was detected, the transmitter microcontroller would trigger the receiver microcontroller to activate a 20 V voltage regulator (Pololu Robotics) to apply a 3-second square-wave pulse.

4.6 Plant Growth Conditions

Venus flytrap plants (*Dionaea muscipula*) were grown in a semi-hydroponic system using sphagnum moss and reverse osmosis water in a temperature-controlled greenhouse environment. The experiments were conducted in a controlled environment where the temperature and humidity were kept constant and monitored every minute using a PulsePro environmental monitor. An 86-watt LED grow light maintained a 12 hr:12 hr light-dark cycle.

4.7 Environmental Monitoring Experiments

4.8 Insect Experiments

Healthy large crickets (*Acheta domesticus*) were purchased from Petco in batches of 15 crickets and kept in an enclosure with damp cotton balls for water and Fluker's Orange Cube Cricket Diet for food. The potential of the VFT during the experiments involving crickets was monitored using a Keithley DMM6500 multimeter, measuring the voltage between a bioelectrode and a needle in the hydrated sphagnum moss growing media.

4.8.1 Temperature Variation Experiments

APs were recorded using a Keithley DMM6500 multimeter to monitor the voltage of a bioelectrode on the inside of a VFT lobe and a needle in the hydrated sphagnum moss growing media. Environmental conditions, including temperature, humidity, and light intensity, were monitored using a PulsePro environmental logger, with data collected every minute.

4.9 Imaging

Optical photographs were taken with an iPhone 12 Pro, a Canon EOS Rebel T8i, and a Nikon D7000. Video monitoring of the VFTs during long-term experiments was conducted using a WYZE Cam v3. Images pulled from videos of experiments in Figure 4 were upscaled using Gigapixel AI, and the images from videos of experiments in Figure 5 were upscaled using Upscayl AI Image Upscaler.

Supplementary information. Supplementary information is included in a separate document.

Acknowledgments. This work was supported by the NSF Signals in the Soil Program (Award No. 1935594), and the NSF Graduate Research Fellowship Program (Award No. DGE2040434). Graphical abstract design by Karen Thiebes at Simplified Science Publishing, LLC. Photography consultation and support provided by Ashley Crichton Photography.

Declarations

The University of Colorado-Boulder and the authors E.B., E.J.S., and G.L.W. have filed a patent application related to electronic cryogels. The remaining authors declare no competing interests.

References

[1] Ghafar-Zadeh, E., Forouhi, S., Azadmousavi, T.: Advances in electronic biosensors. In: Advanced CMOS Biochips: Design and Fabrication, pp. 197–224. Springer, ??? (2024)

[2] Sunwoo, S.-H., Han, S.I., Joo, H., Cha, G.D., Kim, D., Choi, S.H., Hyeon, T., Kim, D.-H.: Advances in soft bioelectronics for brain research and clinical neuroengineering. Matter **3**(6), 1923–1947 (2020)

[3] Kaushal, J.B., Raut, P., Kumar, S.: Organic electronics in biosensing: a promising frontier for medical and environmental applications. Biosensors **13**(11), 976 (2023)

[4] Bihar, E., Strand, E.J., Crichton, C.A., Renny, M.N., Bonter, I., Tran, T., Atreya, M., Gestos, A., Haseloff, J., McLeod, R.R., *et al.*: Self-healable stretchable printed electronic cryogels for in-vivo plant monitoring. npj Flexible Electronics **7**(1), 48 (2023)

[5] Im, H., Lee, S., Naqi, M., Lee, C., Kim, S.: Flexible pi-based plant drought stress sensor for real-time monitoring system in smart farm. Electronics **7**(7), 114 (2018)

[6] Kim, J.J., Allison, L.K., Andrew, T.L.: Vapor-printed polymer electrodes for long-term, on-demand health monitoring. Science advances **5**(3), 0463 (2019)

[7] Strand, E.J., Gopalakrishnan, A., Crichton, C.A., Palizzi, M.J., Lee, O., Borsa, T., Bihar, E., Goodrich, P., Arias, A.C., Shaheen, S.E., et al.: Ultrathin screen-printed plant wearable capacitive sensors for environmental monitoring. Advanced Sensor Research, 2400177 (2025)

[8] Volkov, A.G.: Plant Electrophysiology. Springer, ??? (2006)

[9] Fensom, D.: The bioelectric potentials of plants and their functional significance: V. some daily and seasonal changes in the electrical potential and resistance of living trees. Canadian Journal of Botany **41**(6), 831–851 (1963)

[10] Szechyńska-Hebda, M., Lewandowska, M., Karpiński, S.: Electrical signaling, photosynthesis and systemic acquired acclimation. Frontiers in physiology **8**, 684 (2017)

[11] Pachú, J.K., Macedo, F.C., Malaquias, J.B., Ramalho, F.S., Oliveira, R.F., Godoy, W.A., Salustino, A.S.: Electrical signalling and plant response to herbivory: A short review. Plant Signaling & Behavior **18**(1), 2277578 (2023)

[12] Choi, W.-G., Hilleary, R., Swanson, S.J., Kim, S.-H., Gilroy, S.: Rapid, long-distance electrical and calcium signaling in plants. Annual review of plant biology **67**(1), 287–307 (2016)

[13] Johns, S., Hagihara, T., Toyota, M., Gilroy, S.: The fast and the furious: rapid long-range signaling in plants. Plant Physiology **185**(3), 694–706 (2021)

[14] Fabricant, A., Iwata, G.Z., Scherzer, S., Bougas, L., Rolfs, K., Jodko-Władzińska, A., Voigt, J., Hedrich, R., Budker, D.: Action potentials induce biomagnetic fields

in carnivorous venus flytrap plants. Scientific reports **11**(1), 1438 (2021)

[15] Hagihara, T., Mano, H., Miura, T., Hasebe, M., Toyota, M.: Calcium-mediated rapid movements defend against herbivorous insects in mimosa pudica. Nature communications **13**(1), 6412 (2022)

[16] Matsumura, M., Nomoto, M., Itaya, T., Aratani, Y., Iwamoto, M., Matsuura, T., Hayashi, Y., Mori, T., Skelly, M.J., Yamamoto, Y.Y., *et al.*: Mechanosensory trichome cells evoke a mechanical stimuli–induced immune response in arabidopsis thaliana. Nature communications **13**(1), 1216 (2022)

[17] Farmer, E.E., Gao, Y.-Q., Lenzoni, G., Wolfender, J.-L., Wu, Q.: Wound-and mechanostimulated electrical signals control hormone responses. New Phytologist **227**(4), 1037–1050 (2020)

[18] Salvador-Recatalà, V., Tjallingii, W.F., Farmer, E.E.: Real-time, in vivo intracellular recordings of caterpillar-induced depolarization waves in sieve elements using aphid electrodes. New Phytologist **203**(2), 674–684 (2014)

[19] Sukhov, V.: Electrical signals as mechanism of photosynthesis regulation in plants. Photosynthesis Research **130**, 373–387 (2016)

[20] Koziolek, C., Grams, T.E., Schreiber, U., Matyssek, R., Fromm, J.: Transient knockout of photosynthesis mediated by electrical signals. New Phytologist **161**(3), 715–722 (2004)

[21] Guo, X., Liu, D., Chong, K.: Cold signaling in plants: Insights into mechanisms and regulation. Journal of integrative plant biology **60**(9), 745–756 (2018)

[22] Lautner, S., Grams, T.E.E., Matyssek, R., Fromm, J.: Characteristics of electrical signals in poplar and responses in photosynthesis. Plant Physiology **138**(4), 2200–2209 (2005)

[23] Luo, Y., Li, W., Lin, Q., Zhang, F., He, K., Yang, D., Loh, X.J., Chen, X.: A morphable ionic electrode based on thermogel for non-invasive hairy plant electrophysiology. Advanced Materials **33**(14), 2007848 (2021)

[24] Mousavi, S.A., Nguyen, C.T., Farmer, E.E., Kellenberger, S.: Measuring surface potential changes on leaves. nature protocols **9**(8), 1997–2004 (2014)

[25] Volkov, A.G., Vilfranc, C.L., Murphy, V.A., Mitchell, C.M., Volkova, M.I., O'Neal, L., Markin, V.S.: Electrotonic and action potentials in the venus flytrap. Journal of plant physiology **170**(9), 838–846 (2013)

[26] Bakker, J.M., Belterman, C.N., Coronel, R.: Excitability and propagation of the electrical impulse in venus flytrap; a comparative electrophysiological study of unipolar electrograms with myocardial tissue. Bioelectrochemistry **140**, 107810

(2021)

[27] Hedrich, R., Kreuzer, I.: Demystifying the venus flytrap action potential. New Phytologist **239**(6), 2108–2112 (2023)

[28] Senavirathna, M.D.H.J., Muhetaer, G.: Electrode insertion generates slow propagating electric potentials in myriophyllum aquaticum plants. Plant Signaling & Behavior **15**(3), 1734332 (2020)

[29] Meder, F., Saar, S., Taccola, S., Filippeschi, C., Mattoli, V., Mazzolai, B.: Ultraconformable, self-adhering surface electrodes for measuring electrical signals in plants. Advanced Materials Technologies **6**(4), 2001182 (2021)

[30] Volkov, A.G.: Signaling in electrical networks of the venus flytrap (dionaea muscipula ellis). Bioelectrochemistry **125**, 25–32 (2019)

[31] Armada-Moreira, A., Dar, A.M., Zhao, Z., Cea, C., Gelinas, J., Berggren, M., Costa, A., Khodagholy, D., Stavrinidou, E.: Plant electrophysiology with conformable organic electronics: Deciphering the propagation of venus flytrap action potentials. Science Advances **9**(30), 4443 (2023)

[32] Garlando, U., Calvo, S., Barezzi, M., Sanginario, A., Ros, P.M., Demarchi, D.: Ask the plants directly: Understanding plant needs using electrical impedance measurements. Computers and Electronics in Agriculture **193**, 106707 (2022)

[33] Cseresnyés, I., Füzy, A., Kabos, S., Kelemen, B., Rajkai, K., Takács, T.: Monitoring of plant water uptake by measuring root dielectric properties on a fine timescale: diurnal changes and response to leaf excision. Plant Methods **20**(1), 5 (2024)

[34] Bar-On, L., Garlando, U., Singh, H., Avni, A., Sade, N., Zeron, Y., Demarchi, D., Shacham-Diamand, Y.: Plant-based electrical impedance spectroscopy for plant health monitoring. In: Digital Agriculture: A Solution for Sustainable Food and Nutritional Security, pp. 485–517. Springer, ??? (2024)

[35] Volkov, A.G., Adesina, T., Jovanov, E.: Closing of venus flytrap by electrical stimulation of motor cells. Plant signaling & behavior **2**(3), 139–145 (2007)

[36] Volkov, A.G., Carrell, H., Baldwin, A., Markin, V.S.: Electrical memory in venus flytrap. Bioelectrochemistry **75**(2), 142–147 (2009)

[37] Hou, Z., Li, X., Zhang, X., Zhang, W., Wang, Z.L., Zhang, H.: A bioinspired, self-powered, flytrap-based sensor and actuator enabled by voltage triggered hydrogel electrodes. Nano Research **16**(7), 10198–10205 (2023)

[38] Pavlovič, A., Jakšová, J., Novák, O.: Triggering a false alarm: wounding mimics prey capture in the carnivorous venus flytrap (dionaea muscipula). New

Phytologist **216**(3), 927–938 (2017)

[39] Krol, E., Dziubinska, H., Stolarz, M., Trebacz, K.: Effects of ion channel inhibitors on cold-and electrically-induced action potentials in dionaea muscipula. Biologia Plantarum **50**, 411–416 (2006)

Supplementary Files

This is a list of supplementary files associated with this preprint. Click to download.

- VFTSI.pdf
- SIVideo1.mp4
- SIVideo2.mov
- SIVideo3.mp4
- SIVideo4.mp4